Role for β-catenin and HOX transcription factors in *Caenorhabditis elegans* and mammalian host epithelial-pathogen interactions

Javier E. Irazoqui[a,b,c], Aylwin Ng[c], Ramnik J. Xavier[c], and Frederick M. Ausubel[a,b,c,1]

[a]Department of Genetics, Harvard Medical School, and [b]Department of Molecular Biology and [c]Center for Computational and Integrative Biology, Massachusetts General Hospital, Boston, MA 02114

Contributed by Frederick M. Ausubel, September 24, 2008 (sent for review August 8, 2008)

We used the model nematode *Caenorhabditis elegans* infected with the human pathogen *Staphylococcus aureus* to identify components of epithelial immunity. Transcriptional profiling and reverse genetic analysis revealed that mutation of the *C. elegans* β-catenin homolog *bar-1* or the downstream homeobox gene *egl-5* results in a defective response and hypersensitivity to *S. aureus* infection. Epistasis analysis showed that *bar-1* and *egl-5* function in parallel to previously described *C. elegans* immune-response pathways. Overexpression of human homologs of *egl-5* modulated NF-κB-dependent TLR2 signaling in epithelial cells. These data suggest that β-catenin and homeobox genes play an important and conserved role in innate immune defense.

homeobox protein | host-pathogen interactions | *Staphylococcus aureus*

The use of genetically tractable model hosts, including the nematode *Caenorhabditis elegans*, has aided the understanding of host immune defenses (1). A variety of human pathogens infect and kill *C. elegans*, including *Pseudomonas aeruginosa*, and *Staphylococcus aureus*, the latter being a growing major public health concern (1, 2). Previous studies have shown that two highly conserved nematode signaling pathways, the *daf-2*/*daf-16* insulin/IGF1 pathway and the *nsy-1*/*sek-1*/*pmk-1* p38 MAPK pathway, play significant roles in the survival of *C. elegans* during infection (3–6). The p38 MAPK pathway also plays a key role in the mammalian innate immune response (7).

C. elegans lack a circulatory system and known professional immune cells. The principal site of interaction with ingested pathogenic microbes is the lumen of the gut, which is composed of 20 nonrenewable intestinal epithelial cells. Identification and characterization of the components of the *C. elegans* immune response is being actively pursued, in part by monitoring gene expression changes in response to infection (6, 8–10). Recent work has characterized the *C. elegans* transcriptional response to infection by the Gram-negative pathogen *P. aeruginosa*, and highlighted the role of the *nsy-1*/*sek-1*/*pmk-1* pathway during that response (6, 10).

In the work reported here, we find a key role for the evolutionarily conserved transcriptional cofactor *bar-1*/β-catenin in *C. elegans* intestinal epithelial immunity to *S. aureus*. *bar-1*/β-catenin was previously implicated in a number of developmental processes in *C. elegans* as a component of signaling pathways downstream of Wnt secreted glycoprotein ligands (11, 12). We also report here that part of the *bar-1*-dependent response to *S. aureus* is mediated by the effector transcription factor EGL-5, a homeobox protein homologous to the *Drosophila* gene *AbdominalB*. *C. elegans egl-5* controls the development of the posterior end of the animal downstream of Wnt signaling (13–15). Importantly, we also show that human homologs of *egl-5*, which are induced upon *S. aureus* infection in human cells, modulate the activity of the innate immune regulator NF-κB.

Results

DAF-16 and PMK-1 are Not Required for the Induction of Selected *S. aureus*-Responsive Genes. In experiments described elsewhere, we used Affymetrix whole-genome *C. elegans* microarrays to identify 186 genes whose transcription was induced in the early response to *S. aureus* infection, many of which encode proteins predicted to have antimicrobial and detoxification activities (Irazoqui *et al.*, manuscript in preparation). We chose 10 of these *S. aureus*-responsive genes that represented different levels of up-regulation, different degrees of pathogen specificity, and different predicted antimicrobial functions, and verified their induction by using quantitative real-time PCR (qRT-PCR, Fig. 1 *A* and *C*).

We used the set of 10 selected *S. aureus*-induced genes as biomarkers to determine whether two previously identified immune-response pathways, the *pmk-1* p38 MAPK pathway and the *daf-2*/insulin receptor–*daf-16*/FoxO insulin pathway, are involved in the *C. elegans* response to *S. aureus*. Both of these pathways are important for the host response to *P. aeruginosa*, but appear to act in parallel (6). *daf-16* mutants were not affected in the fold induction of any of the 10 selected biomarker genes, except *exc-5* (Fig. 1*A*), which was constitutively de-repressed in *daf-16* mutants (data not shown). Moreover, there were no statistically significant differences in induced levels between wild-type and *daf-16* animals (Fig. 1*B*). These data are similar to previous results showing *daf-16* independence of *P. aeruginosa*-induced genes (6) and consistent with the fact that three different *daf-16* mutants are no more susceptible to *S. aureus* killing than wild type ((4), data not shown). Furthermore, the *daf-16* target genes *lys-7*, *sod-3*, and *mtl-1* were not induced upon *S. aureus* infection and DAF-16 failed to translocate into the nucleus during *S. aureus* (or *P. aeruginosa*) infection [data not shown; (6, 10)], suggesting that DAF-16 is not involved in the host response to these pathogens.

Because *nsy-1*, *sek-1*, and *pmk-1* mutants, corresponding to three kinases in the p38 MAPK cascade, are more susceptible to *S. aureus* infection than wild-type animals [(5); also see below], it was surprising that mutation of *pmk-1* did not significantly affect the fold induction (except *clec-60*, Fig. 1*C*), or the induced levels (Fig. 1*D*) of most of the 10 biomarker genes compared with wild type.

Role of BAR-1/β-catenin and the HOX Gene *egl-5* in the Host Response to *S. aureus*. Because of the potential for cross-talk between immune- and stress-response pathways, our laboratory has explored the role of various stress-related signaling pathways in the *C. elegans* immune response (16). The β-catenin gene *bar-1* was

Author contributions: J.E.I., A.N., R.J.X., and F.M.A. designed research; J.E.I. and A.N. performed research; J.E.I. and A.N. analyzed data; and J.E.I., A.N., R.J.X., and F.M.A. wrote the paper.

The authors declare no conflict of interest.

[1]To whom correspondence should be addressed at: Department of Molecular Biology, Massachusetts General Hospital, Simches Research Building, 185 Cambridge Street CPZN7250, Boston, MA 02114. E-mail: ausubel@molbio.mgh.harvard.edu.

This article contains supporting information online at www.pnas.org/cgi/content/full/0809527105/DCSupplemental.

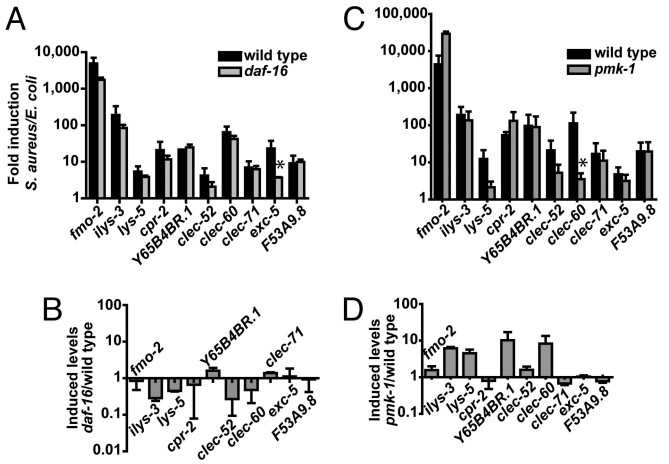

Fig. 1. Mutation of *daf-16* or *pmk-1* does not affect the induction of selected *S. aureus*-induced genes. qRT-PCR analysis showing fold induction (*A*) and final induced levels (*B*) after 8 h *S. aureus* infection in *daf-16*(*mgDf47*) mutant animals, and fold induction (*C*) and final induced levels (*D*) in *pmk-1*(*km25*) mutant animals. Data are the means of two biological replicates, each replicate measured in duplicate and normalized to a control gene, expressed as the ratio of the corresponding *S. aureus*-induced levels and the basal *E. coli* levels (*A* and *C*; a fold induction of 1 indicates no induction) or expressed as the ratio of the corresponding *S. aureus*-induced levels in the mutant and the wild type (*B* and *D*, a ratio of 1 indicates no difference with wild type). Top and bottom panels are from the same time points. Error bars, SEMs. Asterisks represent $P \leq 0.05$.

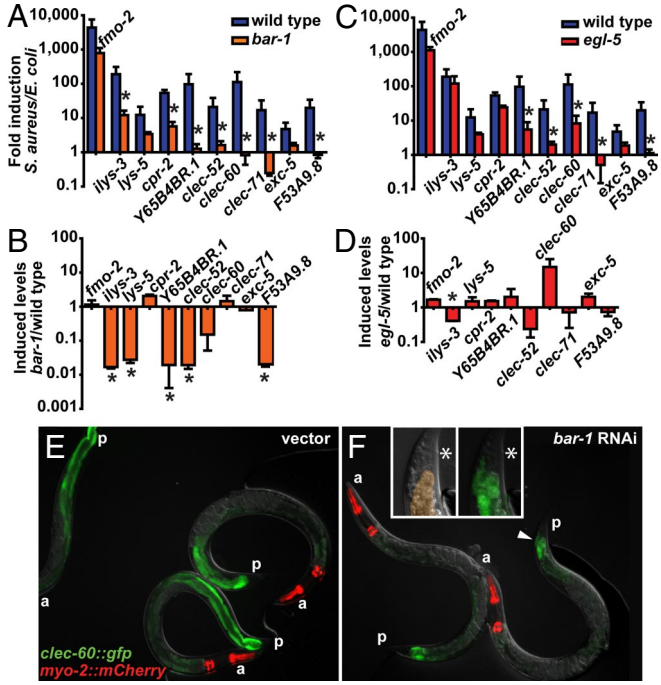

Fig. 2. *bar-1* and *egl-5* are required for the host response to *S. aureus* infection. qRT-PCR analysis of wild type and mutant animals infected with *S. aureus* for 8 h. (*A*) Fold induction levels and (*B*) final expression levels after infection in *bar-1*(*ga80*) versus wild type. (*C*) Fold induction levels and (*D*) final expression levels after infection in *egl-5*(*n486*) versus wild type. Asterisks denote $P \leq 0.05$. Top and bottom panels are from the same time points. (*E* and *F*) Induction of *clec-60*::*gfp* is *bar-1*-dependent. *clec-60*::*gfp* animals were treated with empty vector (*E*) or *bar-1* RNAi (*F*) and subsequently infected during 12 h with *S. aureus*. Inserts show a higher magnification of the area indicated with an arrowhead. Left panel, DIC micrograph showing intestinal cells highlighted in orange. Right panel, overlay DIC and fluorescence micrograph showing GFP leakage into the body cavity. Asterisk indicates the anus. (a) anterior end. (p) posterior end.

recently shown to be involved in the *C. elegans* response to oxidative stress (17). As an initial step to identify novel immunity-related pathways, we tested the induction of the 10 *S. aureus*-activated biomarker genes described above in a *bar-1* mutant background. We found that for seven of the 10 biomarker genes, the fold induction in *bar-1* mutants was lower compared with wild type (Fig. 2*A*). This defective response resulted in dramatically lower induced transcript levels in the *bar-1* mutant for six of the 10 biomarker genes (Fig. 2*B*). The lack of induction of *clec-60* and *F53A9.8* was also observed using *bar-1* RNAi to knock down *bar-1* expression in GFP transcriptional reporter strains (Fig. 2 *E* and *F*, data not shown). Consistent with the gene expression defect shown in Fig. 2, *bar-1* mutant animals were significantly more sensitive to *S. aureus*-mediated killing than wild type (Fig. 3*A*), and *S. aureus*-elicited anal swelling was absent in *bar-1* mutants (data not shown). The requirement for *bar-1* activity appeared to be at least in part post-developmental, because RNAi-mediated knockdown of *bar-1* in adult animals caused a modest but significant increase in susceptibility to *S. aureus*-mediated killing (see supporting information (SI) Fig. S1*D*). Moreover, a functional BAR-1::GFP fusion construct (18) was transiently induced in the posterior gut early during *S. aureus* infection (Fig. S1 *A–C*).

To determine whether the transcriptional activity of *bar-1* is required for defense, we examined loss of function mutants in three *C. elegans* homeobox (HOX) transcription factor genes, *lin-39*, *mab-5*, and *egl-5*, previously identified as downstream mediators of *bar-1*-dependent signaling (18, 19). *egl-5* null mutants (but not *lin-39* or *mab-5* mutants) were more susceptible to *S. aureus* killing than wild type (Fig. 3*B* and Fig. S2 *A* and *B*) and exhibited reduced induction of five of the 10 biomarker genes (Fig. 2*C*). However, the induction defect in the mutant resulted in statistically significant decreased induced expression only of *ilys-3* (and maybe *clec-52*, Fig. 3*D*), because of higher constitutive expression of the other four genes in the mutant (data not shown).

Pathogenicity-Related Phenotypes of *bar-1* and *egl-5* Mutants. Mutants with defects in pharyngeal grinding or defecation exhibit increased susceptibility to killing by *P. aeruginosa* (20). In contrast, the susceptibility of *bar-1* and *egl-5* mutants to *S. aureus* is not likely a consequence of a grinding defect or constipation. *bar-1* and *egl-5* mutant animals variably accumulated *S. aureus* more rapidly than wild type in their intestinal lumina (Fig. S3 *A–C*), but did not accumulate *E. coli* (Fig. S3*D*). Defecation-defective mutants *aex-2*(*sa3*) and *unc-25*(*e156*) were not more susceptible than wild type to *S. aureus* infection (Fig. S2*C*), and *aex-2*(*sa3*) did not accumulate more *S. aureus* than wild type (data not shown).

Epifluorescence and transmission electron microscopy of *bar-1* mutants infected with *S. aureus* revealed leakage of cytoplasmic contents into the body cavity (Fig. 2*F Inset*) and severely damaged intestinal cells (Fig. 4*A*), suggesting more severe *S. aureus*-elicited gut degradation than in wild type (Fig. 4*E*). The microvilli in *bar-1* animals were significantly shortened or were completely absent on the intestinal cell apical surface. In contrast to wild type, we did not observe lysed bacterial cells in the intestinal lumen in the *bar-1* mutants; on the contrary, the bacteria appeared to be undergoing active division, as evidenced by readily observable septa (Fig. 4*A*). These phenotypes were not a consequence of gross malformations of the intestine in the *bar-1* mutants, because *bar-1* animals feeding on *E. coli* exhibited a normal overall intestinal ultrastructure (Fig. 4*B*).

Interestingly, the phenotype of infected *bar-1* mutants was more severe than that of infected *pmk-1* mutants (compare Fig. 4 *A* and *C*). In contrast to *bar-1* animals, *pmk-1* animals contained lysed as well as live dividing bacterial cells. This

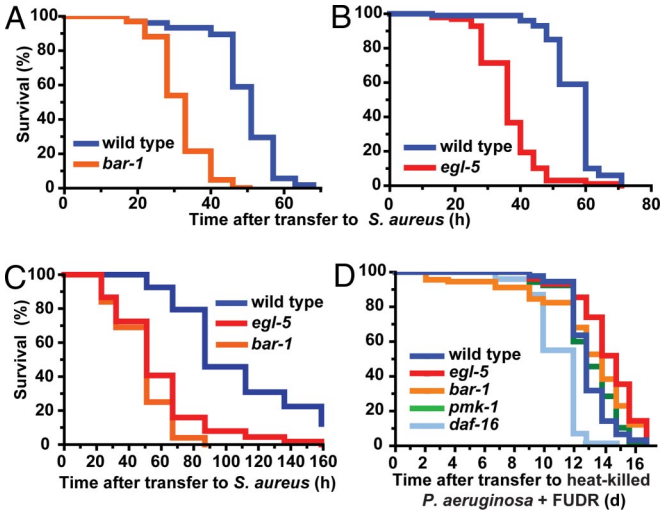

Fig. 3. *bar-1* and *egl-5* mutants are more susceptible to *S. aureus*-mediated killing than wild type. (*A*) *S. aureus*-mediated killing. *bar-1* med. surv. = 33 h, $n = 102$, $P < 0.0001$; wild type med. surv. = 51 h, $n = 105$. (*B*) *S. aureus*-mediated killing. *egl-5* med. surv. = 36 h, $n = 98$, $P < 0.0001$; wild type med. surv. = 60 h, $n = 99$. (*C*) *S. aureus* killing after knockdown of *cdc-25* to prevent progeny production. Wild type med. surv. = 87 h, $n = 94$; *bar-1* med. surv. = 51 h, $n = 100/12$, $P < 0.0001$; *egl-5* med. surv. = 51 h, $n = 113$, $P < 0.0001$. (*D*) Lifespan on heat-killed *P. aeruginosa* PA14 with FUDR. Wild type med. surv. = 12.83 d, $n = 91/5$; *egl-5* = 14.83 d, $n = 98$, $P < 0.0001$; *bar-1* = 13.88 d, $n = 89$, $P = 0.0079$; *pmk-1* = 12.83 d, $n = 105$, $P = 0.3211$; *daf-16* = 11.96 d, $n = 100$, $P < 0.0001$ for comparison with wild type.

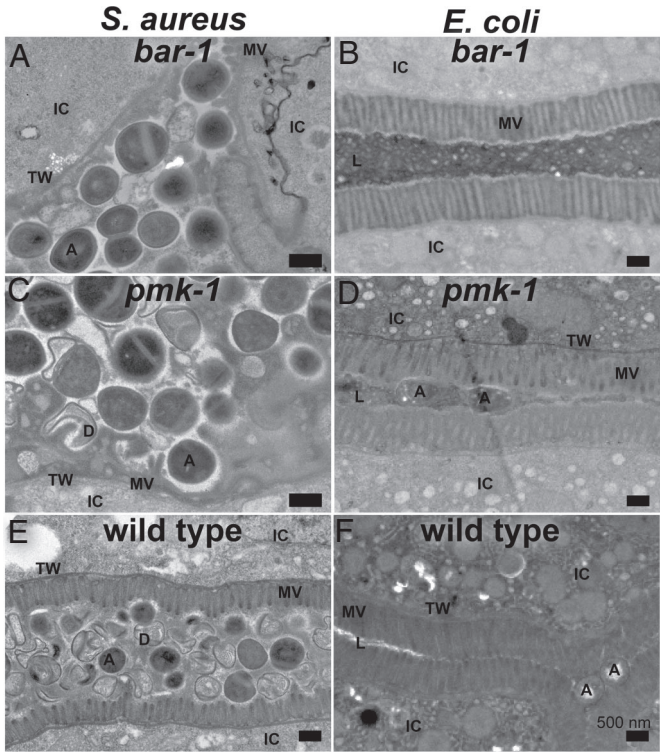

Fig. 4. *bar-1* mutant animals exhibit more severe degradation of intestinal cells 12 h after infection with *S. aureus*. Transmission electron micrographs (TEM) of transversal midbody sections of (*A*) a *bar-1*(*ga80*) mutant animal infected with *S. aureus*, (*B*) an *E. coli*-fed *bar-1*(*ga80*) mutant animal, (*C*) a *pmk-1*(*km25*) mutant animal infected with *S. aureus*, (*D*) an *E. coli*-fed *pmk-1*(*km25*) mutant animal, (*E*) a wild-type animal infected with *S. aureus* for 12 h, and (*F*) an *E. coli*-fed wild type animal. In all *E. coli*-fed controls, occasionally bacterial cells were observed in the lumen mostly occupied by debris. MV, Microvilli; IC, intestinal cells; TW, terminal web; A, live and D, dead bacterial cells; L, intestinal lumen. (Scale bars, 500 nm.)

correlates with the observation that *bar-1* and *egl-5* mutants were more susceptible to *S. aureus* than *pmk-1* mutants (Fig. 5 *A* and *B*). This relationship was reversed during infection by *P. aeruginosa* (Fig. S2*D*), indicating that the *pmk-1*/p38 MAPK pathway is more important for conferring resistance to *P. aeruginosa* than it is for conferring resistance to *S. aureus*, and vice versa for the *bar-1*/*egl-5* pathway.

In previous studies, it was noted that many bacterial pathogens elicit an egg-laying-defective (Egl) phenotype, causing some eggs to hatch within the mother's uterus and resulting in matricide, known as "bagging" (3, 5). However, the enhanced susceptibility of *bar-1* and *egl-5* mutants to pathogen infection is not simply a consequence of constitutive bagging. Both *egl-5* and *bar-1* mutants were more susceptible than wild type to *P. aeruginosa*-mediated killing in the presence of FUDR, which blocks embryonic development and allows the evaluation of phenotypes masked by bagging [Fig. S2*D*, (21)]. Because FUDR inhibits *S. aureus* growth and prevents *S. aureus*-mediated killing, for *S. aureus* killing assays we blocked bagging by sterilizing *bar-1* and *egl-5* worms with *cdc-25* RNAi (10) and found that they were significantly more susceptible to *S. aureus* killing than equally treated wild type (Fig. 3*C*). Conversely, RNAi knockdown of *bar-1* in several sterile mutant backgrounds, including *spe-9*;*fer-15*, caused markedly increased susceptibility to *S. aureus* (Fig. S2*E*). Finally, the decreased lifespan of *bar-1* and *egl-5* mutants on nonpathogenic *E. coli* because of bagging (Fig. S4*A*) was rescued almost entirely in the presence of FUDR (Fig. S4*B*) and *bar-1* and *egl-5* mutants had approximately wild-type longevity when feeding on heat-killed *P. aeruginosa* in the presence of FUDR (Fig. 3*D*). These experiments confirm that the egg-laying defect in *bar-1* and *egl-5* mutants is separable from their defect in innate immunity.

Interaction of the BAR-1 and DAF-2 Pathways. We next used epistasis analysis to determine whether *bar-1* and *egl-5* are components of the previously studied insulin DAF-2/DAF-16 pathway. *bar-1* RNAi completely suppressed the *daf-2*(-) resistance to *S. aureus* down to the level of the *bar-1* RNAi-treated wild type (Fig. S4*C*), suggesting that *bar-1* may function downstream of *daf-2*. However, because loss of *daf-16* by mutation or RNAi only suppressed *daf-2* resistance to the level of wild type [Fig. S4*C*, (4)], because mutation of *bar-1* or *egl-5* did not cause major changes in *daf-16* target gene expression in a *daf-2*(+) background (Fig. S4*D*), and because *daf-16* did not affect the induction of *S. aureus*-response genes (Fig. 1 *A* and *B*), we conclude that it is unlikely that *bar-1* and *egl-5* function in a linear pathway with *daf-16*. This conclusion is similar to previously published data showing that although loss of *pmk-1* suppressed the resistance phenotype of *daf-2* mutants, *pmk-1* and *daf-2*/*daf-16* function in parallel pathways (6). As in the case of *pmk-1*, it is possible that activation of other defense pathways is insufficient for resistance to *S. aureus* in the absence of *bar-1*.

BAR-1 and EGL-5 Act in Parallel to PMK-1/p38 MAPK. We also carried out epistasis analysis to determine whether *bar-1* and *egl-5* function as part of the *tir-1*/*nsy-1*/*sek-1*/*pmk-1* p38 MAPK signaling pathway. *pmk-1*;*bar-1* double mutants were more susceptible than either single mutant (Fig. 5*A*). Likewise, the phenotype of the *egl-5*;*pmk-1* double mutant was stronger than that of either single mutant (Fig. 5*B*). These results suggest that *bar-1* and *egl-5* act in parallel to the *pmk-1* pathway.

Further support for this conclusion was provided by analysis of PMK-1 activation via phosphorylation (3). Significantly, loss of neither *bar-1* nor *egl-5* caused a significant change in PMK-1

IMMUNOLOGY

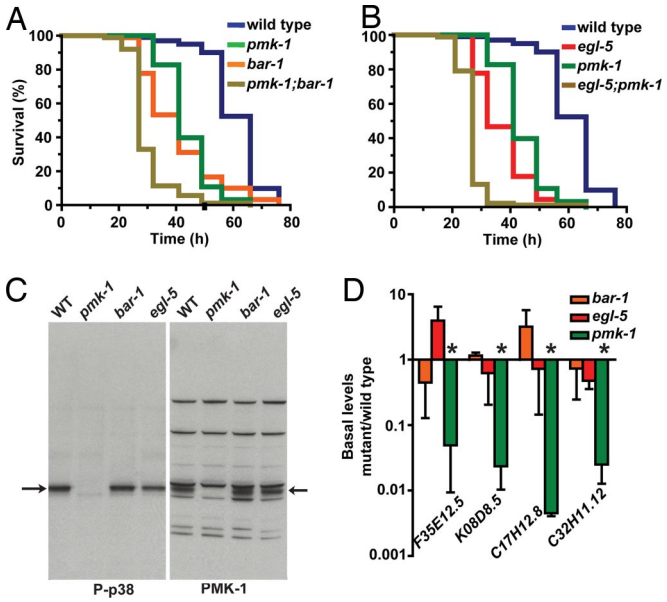

Fig. 5. *bar-1*, *egl-5* function in parallel to *pmk-1*. (*A* and *B*) *S. aureus* killing assays. (*A*) Med. surv. *pmk-1;bar-1* = 27 h, n = 88/6; *bar-1* = 41 h, n = 89/15, $P < 0.0001$; *pmk-1* = 41 h, n = 93/2, $P < 0.0001$ for comparison with double mutant. Although slightly in this assay, *bar-1* mutants were significantly more susceptible than *pmk-1* mutants in most assays (data not shown). (*B*) Med. surv. *egl-5;pmk-1* = 27 h, n = 91/5; *egl-5* = 32 h, n = 90/2, $P < 0.0001$; *pmk-1* = 41 h, n = 93/2, $P < 0.0001$ for comparison with double mutant). Wild type and *pmk-1* data are the same as in *A*. (*C*) Western blot of whole animal lysates from wild type (WT), *pmk-1*(*km25*), *bar-1*(*ga80*), and *egl-5*(*n486*) animals. Similar results as those obtained with the *pmk-1* mutant were also obtained with the *sek-1*(*ag1*) mutant, as previously published (data not shown). Left, anti-phospho-p38 immunoblot. Right, total PMK-1 immunoblot using anti-PMK-1 antiserum. Arrows indicate the 44 kDa band corresponding to PMK-1. Other bands are nonspecific background. (*D*) qRT-PCR in wild type, *bar-1*(*ga80*), *egl-5*(*n486*), and *pmk-1*(*km25*) strains, normalized to a control gene, and presented as ratios with wild type. Asterisks indicate $P \leq 0.05$.

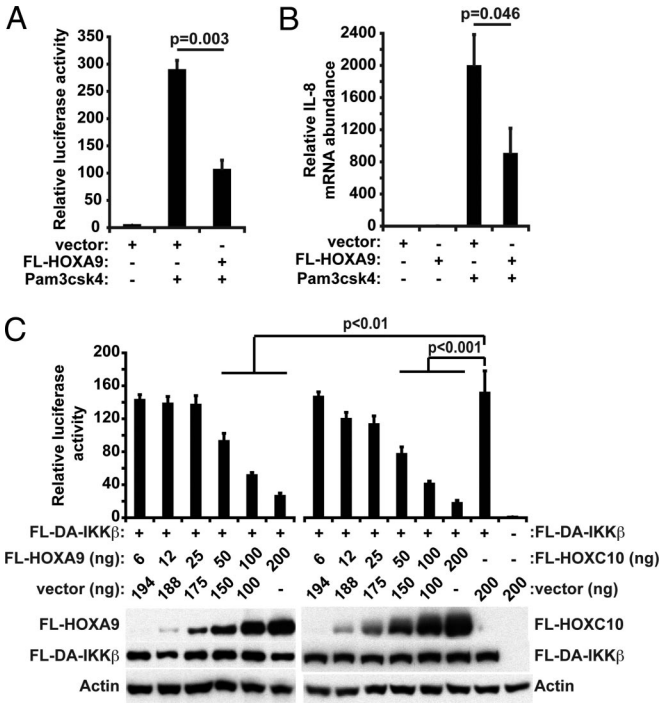

Fig. 6. Up-regulation of HOX genes inhibits NF-κB -dependent TLR2 signaling. Overexpression of human HOXA9 inhibits Pam3csk4-elicited NF-κB reporter (*A*) and IL-8 (*B*) induction. HEK293-TLR2 cells transfected with NF-κB reporter vector were stimulated (or mock-stimulated) with Pam3csk4 for 6 h. Data are mean values of relative luciferase activity normalized to Renilla luciferase acitivity from duplicate experiments ± SD (*A*) or mean values from qRT-PCR measurements of IL-8 transcript levels (relative to GAPDH and the unstimulated vector control) from duplicate experiments ± SD. (*C*) Overexpression of human HOXA9 or HOXC10 inhibits NF-κB activity induced by constitutively active IKKβ. HEK293 cells were transfected with 3x*FLAG-HOXA9* or *HOXC10*, constitutively active IKKβ, NF-κB-luciferase (NF-κB-luc), and empty vectors as indicated. All samples were also transfected with Renilla luciferase vector for normalization. Bottom panel, western blot detection of 3xFLAG-tagged HOXA9 and HOXC10, FLAG-IKKβ, and actin in lysates used for the reporter assay.

activation in whole animal lysates, suggesting that *bar-1* and *egl-5* do not act upstream of *pmk-1* (Fig. 5*C*). As an additional measure of PMK-1 activity, we determined the transcript levels of several genes that require PMK-1 for expression (6). Consistent with the western blot analysis, the expression levels of these genes were reduced in the *pmk-1* but not the *bar-1* and *egl-5* mutants (Fig. 5*D*). Furthermore, loss of *bar-1* or *egl*-5 did not affect the *P. aeruginosa*-elicited induction of *pmk-1*-dependent genes (*C32H11.1*, *F49F16*, and *K08D8.5*), but modestly affected the *pmk-1*-independent gene *T24C4.4* (Fig. S4*E*). These results suggest that neither *bar-1* nor *egl-5* are required for signaling downstream of *pmk-1*. It is also unlikely that *pmk-1* functions upstream of *bar-1* and *egl-5*, because loss of *pmk-1* did not affect the *S. aureus*-elicited induction of any *bar-1*- or *egl-5*-dependent genes (Figs. 1*D* and 3 *A* and *C*). Thus, we conclude that *bar-1*/*egl-5* function in parallel to *pmk-1* during the response to infection.

Human Homologs of EGL-5 Regulate NF-κB Signaling. To identify human homologs of EGL-5 potentially associated with innate immunity in the context of *S. aureus* infection, we evaluated publicly available microarray data of human polymorphonuclear neutrophils (PMNs) infected with *S. aureus in vitro* (22). We found that *S. aureus* infection induced a number of key genes of the inflammatory and innate immune responses, including proinflammatory cytokines and chemokines (e.g., *IL1B, IL8, IL12B*, and *TNF*) and components of the Toll (e.g., *TLR2, IRAK1, NFKBIA*, and *NFKB1*) and MAP kinase pathways (e.g., *MAP2K3* and *DUSP3*) (Fig. S5*A*). Additionally, a number of Wnt signaling genes (e.g., *WNT2B, FZD3, FZD6, TCF2, TCF4, TCF7L1*, and *TCFL5*) and HOX genes (*HOXA5*, *HOXA9*, *HOXB5*, *HOXB9*, *HOXC10*, and *HOXD1*) exhibited similar expression profiles (Fig. S5*A*). Network analysis using protein interaction data suggested the possible involvement of the EGL-5 homolog *HOXA9* in the Toll-like receptor 2 (TLR2) signaling pathway, which is essential for *S. aureus* recognition (Fig. S5*B*).

To determine the function of HOX expression in TLR2 signaling, we measured Pam3csk4-elicited NF-κB activation in human epithelial-TLR2 reporter cell lines expressing HOXA9 (see Methods). Overexpression of *HOXA9* inhibited Pam3csk4-induced transcription of an NF-κB reporter (Fig. 6*A*) and IL-8 (Fig. 6*B*). This suggested that HOXA9 may dampen NF-κB -dependent TLR2 signaling, consistent with a recent report (23). Furthermore, the induction of the NF-κB reporter by constitutively active IKKβ was inhibited by HOXA9 in a dose-dependent manner (Fig. 6*C*), suggesting that HOXA9 functions at the level of or downstream of NF-κB. We observed similar results with HOXC10 (Fig. 6*C*), showing the potential for multiple *egl-5* homologues to modulate NF-κB redundantly. These data suggest that multiple human HOX proteins may play a role in the innate immune response to *S. aureus* infection as modulators of NF-κB -dependent transcription.

Discussion

We show here that *bar-1*/β-catenin, which is involved in many processes during *C. elegans* development, is also required postde-

velopmentally to induce genes that respond to *S. aureus* infection. *egl-5*, a HOX gene previously shown to act downstream of *bar-1* in the development of the nematode posterior end, is also required for the proper response to *S. aureus* infection. Mutation of *bar-1* or *egl-5* results in enhanced susceptibility to pathogenic attack. Importantly, *bar-1* and *egl-5* appear to operate in a novel pathway that is distinct from the *C. elegans daf-2/daf-16* insulin and the *tir-1/pmk-1* p38 MAPK signaling pathways.

Although the molecular mechanism underlying *bar-1* and *egl-5* function during the response to infection is unknown, one possibility is that *bar-1*-mediated transcriptional activation of immune effector genes, including *egl-5*, results directly in enhanced resistance. *bar-1* RNAi in adult animals caused modest sensitivity to *S. aureus* and BAR-1 protein levels increased transiently in adults upon infection, supporting this view. Unfortunately, heat-shock induced overexpression of *bar-1* or *egl-5* negatively affects viability, precluding a direct experimental test of this hypothesis [data not shown, (15)]. Alternatively, *bar-1/egl-5* could be involved in the development of a tissue that is required for the detection of *S. aureus* infection. These two scenarios are not mutually exclusive.

When comparing biomarker expression on *S. aureus* vs. *E. coli*, the profiles of the *bar-1* and *egl-5* mutants are similar (Fig. 2 *A* and *C*), which supports the notion that they function in the same pathway. The levels of most biomarker genes were strikingly reduced in *bar-1* mutants exposed to *S. aureus* (Fig. 2*B*), but were relatively unaffected in *egl-5* animals (Fig. 2*D*), even though *bar-1* and *egl-5* animals are equally susceptible to *S. aureus*. The reason for this apparent discrepancy is that most of these biomarker genes are constitutively derepressed in the *egl-5* mutant (data not shown), suggesting that *egl-5* may act as a negative regulator, although it is also possible that *egl-5* is required for the expression of immune effectors not included in our biomarker set. These complex gene expression patterns imply sophisticated regulatory mechanisms and likely involve several signaling pathways acting in concert (Fig. S6). Recent work showed that *egl-5* is required for the swelling response to the nematode-specific pathogen *Microbacterium nematophilum*, although the molecular mechanism of *egl-5* action remains unclear (24). This result is in agreement with our results showing an important role for *egl-5* in the host response to infection.

We found that a BAR-1::GFP translational fusion is faintly expressed throughout the body, with highest expression in the posterior gut, consistent with reports that *egl-5* also is expressed and functions in the posterior end (14, 19, 25). Interestingly, the three *bar-1*-dependent biomarker genes we tested (*clec-52*, *-60*, and *F53A9.8*) are more highly expressed in the posterior intestine. Thus, *bar-1/egl-5* may act in response to *S. aureus* infection in a local manner to induce the expression of genes in the posterior end of the animal. Unfortunately, our attempts to determine the tissue-specific requirements of *bar-1* and *egl-5* in immunity by rescuing the *bar-1* mutant using various tissue-specific promoters have so far been unsuccessful, despite clear rescue of the vulval morphogenesis phenotype by ectopic and hypodermal expression constructs (data not shown).

Seventy percent of 186 genes up-regulated by *S. aureus* infection did not overlap with genes up-regulated during either *P. aeruginosa* or *M. nematophilum* infection (Irazoqui *et al.* manuscript in preparation). This indicates that a large component of the transcriptional host response to infection is pathogen-specific, consistent with recent reports using other approaches (8, 26). Our data show a correlation between the severity of host-response defects and susceptibility to killing, such that *bar-1* and *egl-5* mutants are more susceptible to *S. aureus*, whereas *pmk-1* mutants are more susceptible to *P. aeruginosa*. Thus, *C. elegans* may defend itself against infection via pathogen-specific defense response pathways (Fig. S6).

Recent work has shown that β-catenin is transiently activated in human epithelia after stimulation by bacteria (27, 28), but the functional consequences of this induction remain unclear. Our work and that of others show that the long-term stabilization of β-catenin can lead to down-regulation of NF-κB, causing the loss of expression of some NF-κB target genes; for example, IL-8 and κB-element based reporters, but not others (e.g., TRAF1, FAS, and CRP) [data not shown, (28, 29)]. Moreover, the data from our *C. elegans* model suggest the involvement of β-catenin in the regulation of pathogen-response genes independently of NF-κB [*C. elegans* does not have an NF-κB ortholog (30)] and recent evidence suggests this may also be the case in mammalian intestinal epithelia (31–34).

Like *egl-5* in nematodes, HOX proteins downstream of β-catenin (35) may be required for the induction of pathogen-response genes in humans. Given the greatly expanded HOX gene clusters in humans, it is possible that several HOX proteins exert this function redundantly. We show that HOXA9 and HOXC10, two HOX proteins induced by stimulation with *S. aureus*, can modulate NF-κB in human epithelial cells, consistent with recent reports (36). Previous data also show that HOXA9 is required for the expression of immunity-related genes (37, 38).

Finally, because a fully functional NF-κB pathway is absent in nematodes and because nematodes and humans share a conserved immune function for β-catenin and HOX signaling, we hypothesize that β-catenin-dependent innate immune pathways may have evolved earlier than NF-κB signaling pathways. Subsequently, with the acquisition of the TLR/NF-κB axis in arthropods, the β-catenin/HOX pathway may have been recruited to modulate NF-κB signaling.

Materials and Methods

Strains. *C. elegans* strains used in this study are detailed in Table S1. Bacterial strains are detailed in Table S2.

Infection and Lifespan Assays. *S. aureus* and *P. aeruginosa* killing assays were conducted at least twice, as described (5, 6). *P. aeruginosa* assays were supplemented with 80–100 μg/ml 5-fluorodeoxyuridine (FUDR, Sigma). Data are median survival, N (number of deaths/censored) and *P* value. A *P* value less than or equal to 0.05 was considered significantly different from control. Lifespan assays were performed at least twice, as described (6). For experiments using heat-killed PA14, overnight cultures of bacteria were concentrated and incubated at 95°C for 30 min. Plates were supplemented with 80–100 μg/ml FUDR and 100 μg/ml kanamycin.

Quantitative RT-PCR Analysis. Synchronized *C. elegans* animals were treated essentially as for killing assays described above, omitting FUDR. For *S. aureus* assays, infected samples were compared with parallel samples feeding on heat-killed *E. coli* OP50 on the same medium. Total RNA was extracted as described (6) and reverse transcribed by using the SuperScript III kit (Invitrogen). cDNA was subjected to qRT-PCR analysis as described (6). Primer sequences are detailed in Table S3. All values are normalized against the control gene *snb-1*, which did not vary under conditions being tested. Fold change was calculated by using the Pfaffl method (39). One-sample t tests were performed by using Graphpad Prism 4. A *P* value less than or equal to 0.05 was considered significant. Total *HEK293-TLR2* RNA was reverse-transcribed by using the iScript cDNA synthesis kit (Bio-Rad). Real-time quantitative PCR was performed in the iQ5 detection system (Bio-Rad) by using the iQ-SYBR Green supermix (Bio-Rad). *GAPDH* was used for normalization.

***clec-60* GFP Fusion.** PCR was used to amplify 1,665 bp of DNA upstream of the *clec-60* start site. Details of construction can be found in the *SI Methods*.

RNAi Knockdown. RNAi was carried out by using bacterial feeding RNAi (see *SI Methods* for further details).

Western Blot Analysis of PMK-1 Activation. Synchronized L4 populations of N2 wild type, *bar-1*(*ga80*), *egl-5*(*n486*), and *pmk-1*(*km25*) animals were treated as in (3). Western blot analyses of PMK-1 and activated p38 MAPK were as described (3).

IMMUNOLOGY

NF-κB Reporter Assays. Experimental details can be found in the *SI Methods*.

ACKNOWLEDGMENTS. We thank E. Troemel, L. Stanek, S. Margolis, and D. Colón-Ramos for critical reading of the manuscript and J. Powell for help designing qRT-PCR primers. TEM was performed by M. McKee in the Microscopy Core of the Center for Systems Biology supported by National Institutes of Health Grants DK43351 and DK57521. Nematode strains were provided by the *Caenorhabditis* Genetics Center funded by the National Institutes of Health National Center for Research Resources. This work was funded by National Institutes of Health Grants AI062773 (to R.J.X.) and AI064332 (to F.M.A.) and by postdoctoral fellowships from the Jane Coffin Childs Memorial Fund for Medical Research and the Charles A. King Trust, Bank of America, Co-Trustee (Boston, MA) (to J.E.I.), and from the Crohn's and Colitis Foundation of America (to A.N.).

1. Sifri CD, Begun J, Ausubel FM (2005) The worm has turned–microbial virulence modeled in Caenorhabditis elegans. *Trends Microbiol* 13:119–127.
2. Elston DM (2007) Community-acquired methicillin-resistant Staphylococcus aureus. *J Am Acad Dermatol* 56:1–16.
3. Kim DH, *et al.* (2002) A conserved p38 MAP kinase pathway in Caenorhabditis elegans innate immunity. *Science* 297:623–626.
4. Garsin DA, *et al.* (2003) Long-lived C. elegans daf-2 mutants are resistant to bacterial pathogens. *Science* 300:1921.
5. Sifri CD, Begun J, Ausubel FM, Calderwood SB (2003) Caenorhabditis elegans as a model host for Staphylococcus aureus pathogenesis. *Infect Immun* 71:2208–2217.
6. Troemel ER, Chu SW, Reinke V, Lee SS, Ausubel FM, Kim DH (2006) p38 MAPK regulates expression of immune response genes and contributes to longevity in C. elegans. *PLoS Genet* 2:e183.
7. Matsuzawa A, *et al.* (2005) ROS-dependent activation of the TRAF6-ASK1–p38 pathway is selectively required for TLR4-mediated innate immunity. *Nat Immunol* 6:587–592.
8. Wong D, Bazopoulou D, Pujol N, Tavernarakis N, Ewbank JJ (2007) Genome-wide investigation reveals pathogen-specific and shared signatures in the response of Caenorhabditis elegans to infection. *Genome Biol* 8:R194.
9. O'Rourke D, Baban D, Demidova M, Mott R, Hodgkin J (2006) Genomic clusters, putative pathogen recognition molecules, and antimicrobial genes are induced by infection of C. elegans with M. nematophilum. *Genome Res* 16:1005–1016.
10. Shapira M, Hamlin BJ, Rong J, Chen K, Ronen M, Tan MW (2006) A conserved role for a GATA transcription factor in regulating epithelial innate immune responses. *Proc Natl Acad Sci USA* 103:14086–14091.
11. Eisenmann, DM (2005) Wnt signaling. *WormBook*, ed The C. elegans Research Community, 10.1895/wormbook. 1.7.1.
12. Eisenmann DM, Kim SK (2000) Protruding vulva mutants identify novel loci and Wnt signaling factors that function during Caenorhabditis elegans vulva development. *Genetics* 156:1097–1116.
13. Ferreira HB, Zhang Y, Zhao C, Emmons SW (1999) Patterning of Caenorhabditis elegans posterior structures by the Abdominal-B homolog, egl-5. *Dev Biol* 207:215–228.
14. Chamberlin HM, Brown KB, Sternberg PW, Thomas JH (1999) Characterization of seven genes affecting Caenorhabditis elegans hindgut development. *Genetics* 153:731–742.
15. Jiang LI, Sternberg PW (1998) Interactions of EGF, Wnt and HOM-C genes specify the P12 neuroectoblast fate in C. elegans. *Development* 125:2337–2347.
16. Kim D, *et al.* (2004) Integration of Caenorhabditis elegans MAPK pathways mediating immunity and stress resistance by MEK-1 MAPK kinase and VHP-1 MAPK phosphatase. *Proc Natl Acad Sci USA* 101:10990–10994.
17. Essers MA, de Vries-Smits LM, Barker N, Polderman PE, Burgering BM, Korswagen HC (2005) Functional interaction between beta-catenin and FOXO in oxidative stress signaling. *Science* 308:1181–1184.
18. Eisenmann DM, Maloof JN, Simske JS, Kenyon C, Kim SK (1998) The beta-catenin homolog BAR-1 and LET-60 Ras coordinately regulate the Hox gene lin-39 during Caenorhabditis elegans vulval development. *Development* 125:3667–3680.
19. Maloof JN, Whangbo J, Harris JM, Jongeward GD, Kenyon C (1999) A Wnt signaling pathway controls hox gene expression and neuroblast migration in C. elegans. *Development* 126:37–49.
20. Shapira M, Tan M (2008) Genetic Analysis of Caenorhabditis elegans Innate Immunity. *Methods Mol Biol* 415:429–442.
21. Shaw WM, Luo S, Landis J, Ashraf J, Murphy CT (2007) The C. elegans TGF-beta Dauer pathway regulates longevity via insulin signaling. *Curr Biol* 17:1635–1645.
22. Borjesson DL, Kobayashi SD, Whitney AR, Voyich JM, Argue CM, Deleo FR (2005) Insights into pathogen immune evasion mechanisms: Anaplasma phagocytophilum fails to induce an apoptosis differentiation program in human neutrophils. *J Immunol* 174:6364–6372.
23. Trivedi CM, Patel RC, Patel CV (2007) Homeobox gene HOXA9 inhibits nuclear factor-kappa B dependent activation of endothelium. *Atherosclerosis* 195:e50–60.
24. Gravato-Nobre MJ, *et al.* (2005) Multiple genes affect sensitivity of Caenorhabditis elegans to the bacterial pathogen Microbacterium nematophilum. *Genetics* 171:1033–1045.
25. Chisholm A (1991) Control of cell fate in the tail region of C. elegans by the gene egl-5. *Development* 111:921–932.
26. Alper S, McBride SJ, Lackford B, Freedman JH, Schwartz DA (2007) Specificity and complexity of the Caenorhabditis elegans innate immune response. *Mol Cell Biol* 27:5544–5553.
27. Kumar A, *et al.* (2007) Commensal bacteria modulate cullin-dependent signaling via generation of reactive oxygen species. *EMBO J* 26:4457–4466.
28. Sun J, *et al.* (2005) Crosstalk between NF-kappaB and beta-catenin pathways in bacterial-colonized intestinal epithelial cells. *Am J Physiol Gastrointest Liver Physiol* 289:G129–137.
29. Deng J, *et al.* (2002) beta-catenin interacts with and inhibits NF-kappa B in human colon and breast cancer. *Cancer Cell* 2:323–334.
30. Kurz CL, Ewbank JJ (2003) Caenorhabditis elegans: An emerging genetic model for the study of innate immunity. *Nat Rev Genet* 4:380–390.
31. Cavard C, *et al.* (2006) Overexpression of regenerating islet-derived 1 alpha and 3 alpha genes in human primary liver tumors with beta-catenin mutations. *Oncogene* 25:599–608.
32. van Es JH, *et al.* (2005) Wnt signalling induces maturation of Paneth cells in intestinal crypts. *Nat Cell Biol* 7:381–386.
33. Andreu P, *et al.* (2005) Crypt-restricted proliferation and commitment to the Paneth cell lineage following Apc loss in the mouse intestine. *Development* 132:1443–1451.
34. Wehkamp J, *et al.* (2007) The Paneth cell alpha-defensin deficiency of ileal Crohn's disease is linked to Wnt/Tcf-4. *J Immunol* 179:3109–3118.
35. Klapholz-Brown Z, Walmsley GG, Nusse YM, Nusse R, Brown PO (2007) Transcriptional program induced by Wnt protein in human fibroblasts suggests mechanisms for cell cooperativity in defining tissue microenvironments. *PLoS ONE* 2:e945.
36. Trivedi CM, Patel RC, Patel CV (2008) Differential regulation of HOXA9 expression by nuclear factor kappa B (NF-kappaB) and HOXA9. *Gene* 408:187–195.
37. Bei L, Lu Y, Eklund EA (2005) HOXA9 activates transcription of the gene encoding gp91Phox during myeloid differentiation. *J Biol Chem* 280:12359–12370.
38. Bandyopadhyay S, Ashraf MZ, Daher P, Howe PH, DiCorleto PE (2007) HOXA9 participates in the transcriptional activation of E-selectin in endothelial cells. *Mol Cell Biol* 27:4207–4216.
39. Pfaffl MW (2001) A new mathematical model for relative quantification in real-time RT-PCR. *Nucleic Acids Res* 29:e45.